Cold Spray Copper Coatings for Used Fuel Containers

Peter Keech[1], Phuong Vo[2], Dominique Poirier[2], Jean-Gabriel Legoux[2]
[1] Nuclear Waste Management Organization, Toronto, Ontario, Canada
(pkeech@nwmo.ca)
[2] National Research Council, Boucherville QC, Canada

Abstract

Recently, the Nuclear Waste Management Organization has been developing copper coatings as a method of protecting steel used fuel containers (UFCs) from corrosion within a deep geological repository. The corrosion barrier design is based on the application of a copper coating bonded directly to the exterior surface of the UFC structural core. Copper coating technologies amendable to supply of pre-coated UFC vessel components and application to the weld zone following UFC closure within the radiological environment have been investigated. Copper cold spray has been assessed for both operations; this paper outlines the research and development to date of this technique.

1. Introduction

The Nuclear Waste Management Organization (NWMO) was established in 2002 in accordance with the Nuclear Fuel Waste Act to assume responsibility for the long-term management of Canada's used nuclear fuel. The program's plan implementation will include used fuel retrieval from reactor sites, transportation to the disposal facilities, packaging of the fuel into containers, and placement in an underground Deep Geologic Repository (DGR) (NWMO, 2010). The present approach, shown in Figure 1, envisions the conceptual long term storage of radioactive fuel bundles in specially designed containers for CANDU fuel. The containers would be emplaced in the rock of a suitable geological formation at a minimum of 500 m of depth, for an intended lifespan of more than 100,000 years (i.e., indefinite storage).

A major engineered component of DGR design is the Used Fuel Container (UFC). The UFC consists of an inner container of steel strong enough to withstand geological pressures, including glaciation scenarios, and an outer layer of copper for corrosion resistance. The previous reference concept was based on the Swedish (SKB) and Finnish (POSIVA) containers which are described as a "dual-vessel" design. In this design, the steel inner vessel is contained within a 50 mm thick copper "overpack" outer vessel which is sealed shut via friction stir welding. The size of the reference container is over 4 m in length and 1 m in diameter and is reflective of the dimensional constraints (i.e. length) of SKB/POSIVA's PWR and BWR fuel bundles. When loaded with fuel, this container weighs over 25 tonnes. It should be noted that the dimensions of the copper overpack are not dictated by corrosion allowance requirements but rather manufacturing considerations associated with cylindrical shell fabrication. For corrosion purposes, a much thinner layer of copper is required; a 100,000 year container life can be achieved with less than 0.4 mm of copper. However, the use of conventional pierce/draw or extrusion methodologies to fabricate large copper shells from the extremely large copper ingots requires parts to retain significant strength to avoid collapse during manufacturing; this leads to large thickness dimensions. As a further manufacturing challenge, the requirement of a 1 mm nominal gap between a separately fabricated copper shell and inner steel container must also be met; this requirement is due to copper creep considerations.

In 2012, the NWMO undertook an optimization study to look at both the design and manufacture of its engineered barriers for the DGR. The UFC was assessed in terms of design options available specific to CANDU fuel bundles which are smaller (0.5 m in length) and lighter (25 kg) than PWR/BWR fuel assemblies. From this study, a UFC design (the "Mark II") consisting of a 2.7 tonne used fuel container (~2.5 m length x 0.57 m Ø) with a carbon-steel core, copper-coated surface and welded spherical heads was selected for development. As part of this program, a comprehensive effort was initiated to assess modern, innovative coating technologies for application of a 3 mm design thickness to the exterior surface. Notwithstanding the significant reduction in copper contribution costs associated with the coating concept, the use of integrally bonded coatings has an important engineering performance benefit over the dual-shell, overpack design: namely, it eliminates concerns over creep ductility degradation.

This paper outlines the research work performed so far to develop the cold spray coating technology for this application. After a short review of the cold spray process itself, the initial process optimization trials performed on small coupons are presented, followed by the coating validation on UFC-type materials and subsequent process demonstration through prototyping activities.

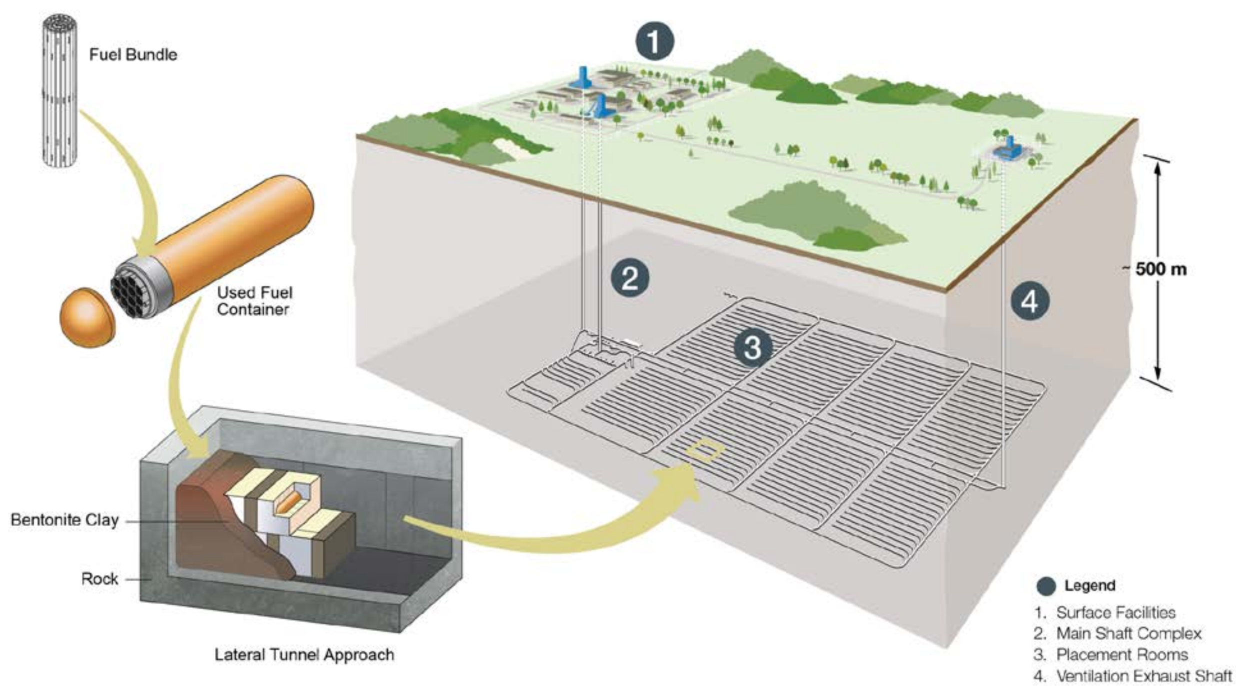

Figure 1: Schematic view of deep geological repository with copper coated "Mark II" UFC.

2. Cold Spray Process

Cold spray is a solid state process that uses a high-speed gas jet to accelerate powder particles toward a substrate where they plastically deform and consolidate upon impact [1]. The process is schematically represented in Figure 2[2]. It consists of a converging/diverging (De Laval) nozzle which enables the generation of supersonic gas flow, a gas heater and powder feeding unit.

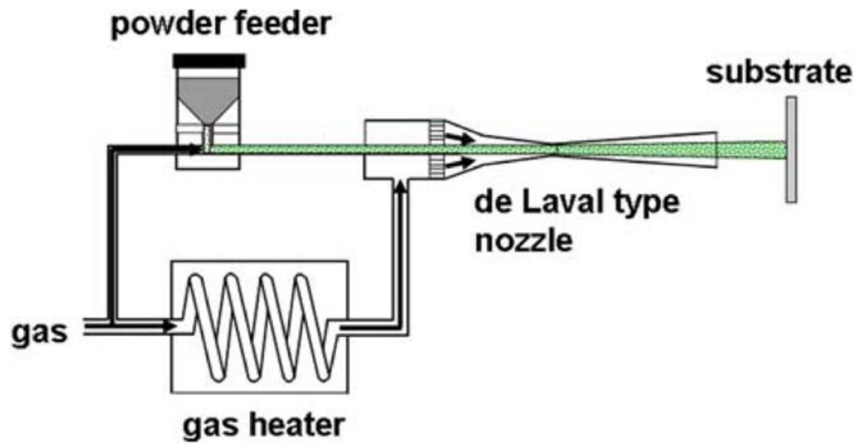

Figure 2: Schematic diagram of cold spray process

Since the particles to be deposited are entrained by the gas flow, the highest gas velocity achievable is typically targeted as the means to move the entrained particle faster. Equation (1) [3] presents the relationship between the gas velocity at the exit of a converging /diverging nozzle as a function of the gas properties and temperature. The Mach number (M) of the nozzle is defined by its geometry. It can be seen that the higher the stagnation temperature (the gas temperature entering the DeLaval nozzle) and the lighter the gas, the higher the velocity (ν) obtained.

$$\boldsymbol{v} = \boldsymbol{M}\sqrt{\frac{\Upsilon R T o}{1+\left(\Upsilon-\frac{1}{2}\right)M^2}} \tag{1}$$

M is the Nozzle Mach number,
Υ is the gas specific heat ratio
R is the universal gas constant
T_0 is the gas stagnation temperature

There are several types of adhesion mechanisms that can lead to a coating. Equation (2) [4] estimates the minimum velocity (called critical velocity (V_{cr})) that needs to be reached in order to form a coating. Dense and adherent coatings are formed at velocities higher than this critical velocity.

$$v_{cr} = 667 - 14\,\rho + 0.08\,T_m + 0.1\,\sigma_u - 0.4\,T_i \tag{2}$$

σ_u ultimate strength (MPa)
ρ density (g/cc)
T_m melting point °C
T_i initial temperature °C

As seen from equation 1, temperature plays an important role in the exit gas velocity and in turn for particle velocity. Pressure and standoff distance are also important factors. Figure 3 shows these effects.

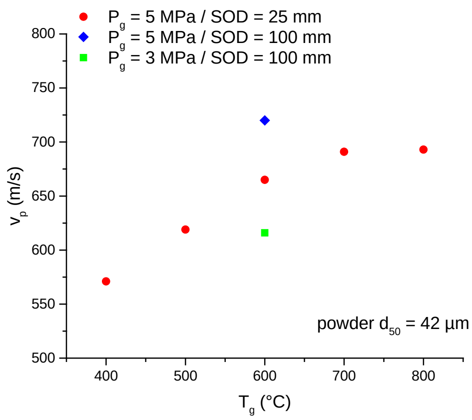

Figure 3: Evolution of particle velocity as a function of the gas temperature for different pressure and standoff distance.

3. Coating Development

Based on structural analysis, preliminary mechanical property requirements for coating performance have been set at a minimum elongation of 10% (ductility) and adhesion strength of 20 MPa. In aid of coating parameter development, values of 15% elongation and 60 MPa adhesion strength were set as a target to achieve sufficient margin. As discussed below, the 60 MPa bond strength is reflective of the ASTM C633 test method whereby failure in the glue (at ~60 MPa) is considered a bounding limit of the test and a conservative go/no-go criterion. In addition to mechanical property requirements, a limit of maximum porosity per unit area of 1 % was also established for metallurgical quality.

Coating development was initiated with Cu powder selection. Among the 8 powders evaluated, a spherical powder displaying low oxygen content, good flowability, generating minimal equipment clogging and producing sound, dense and adherent coatings was selected for further trials. Still, it is worth noting that dense and sound coatings could be produced from most powders studied regardless of their characteristics, which suggests easy powder supply and availability from multiple sources.

A series of trials were performed using typical cold spray setups, and a range of post-deposition heat treatments to develop preliminary specifications. Using dedicated sample holders (Figure 4(a) and (b)), low carbon steel substrates were grit blasted with 24 µm alumina, and spray runs were performed to produce samples on: 25 mm diameter steel puck substrates (Figure 4(c) uncoated, Figure 4(d) coated); and 150 × 150 mm steel plates (Figure 4(e)). Figure 4(f) and Figure 4(g) illustrate substrate coating during operation. Overall, the series of experiments validated the capability of cold spray to produce fully dense copper coatings using a wide range of spray parameters, as measured porosity was less than or equal to 0.4 ± 0.6 % for all coatings.

Figure 4: Cold Spray Development Components, including (a) Puck sample holder; (b) Plate and Puck holder; (c) Steel puck substrate (d) Coated puck samples (e) Steel Plates (f) Process at beginning and (g) Shortly after initiation of Cold Spray Coating.

The particle velocity measurements for 13 different spraying conditions with the mean particle size, d_{50} = 42 µm powder ranged from 570 m/s to 750 m/s, with optimized conditions at the upper end of the measured range. Those values are well within the window of deposition for Cu (~ 400-1100 m/s [2]), explaining the low level of porosity obtained. Spray results are typically closely linked to input parameters, including particle velocity, particle and substrate temperature, as these dramatically affect particle deformation during coating production. Greater deformation of particles is associated, in general, with low coating porosity, high coating cohesion and higher bonding strength. However, defining and getting "good" coating adhesion can be a challenge, and was for this program. While the coating bond strength requirement for the application was initially set at 60 MPa (as measured via ASTM C633 standard testing procedure), bond strength values obtained with N_2 process gas were ranging from 0 to about 30 MPa. In order to maximize coating adhesion and meet the preliminary application requirement, a bond coat sprayed with He was selected, followed by a N_2-sprayed top coat to build the required thickness. The bond coat had the effect of increasing the copper particle velocity, and improving adhesion, above the 60 MPa threshold where glue fails in ASTM C633 testing. Accordingly, the ongoing specification for the coating is 60 MPa (measured via ASTM C633 or equivalent methods).

As-sprayed cold spray samples are brittle and must be annealed to recover ductility. This program included a range of annealing conditions based on the temperatures of stress relieving and annealing of pure wrought copper. Samples were screened through microhardness and microstructure characterization following 1 h annealing at temperatures of 200 °C, 300 °C, 400 °C, 500 °C, and 600 °C. In addition, a 10 h lower temperature (200 °C) was performed. Samples from these were subjected to adhesion, tensile and bend testing according to ASTM standards (ASTM C 633, ASTM E 8 and ASTM E 290, respectively).

Based on the hardness measurements (Figure 5) and microstructure analysis of the micrograph coupons in screening tests (not shown), the following two optimized annealing conditions were initially identified: 1 h at 300 °C and 1 h at 600 °C. 300°C featured a relatively low temperature that produced a significant decrease in hardness from the as-sprayed condition, as shown in Figure 5, while 600°C produced microstructural restoration (i.e. recrystallization) in the annealed coating.

As expected, stress-strain curves for coatings in the as-sprayed and annealed conditions, revealed that annealing decreased coating strength and increased ductility, with a greater effect obtained at higher temperature, Figure 6. The ~16% that was obtained at 300°C (not shown) was close to the minimum project target value of 15%; thus subsequent efforts focused at slightly higher temperatures. Heat treatments of coatings for 1 h at 350 °C and 400 °C produced increases in ductility values to 23.2 ± 3.0 % and 25.9 ± 6.6 %, respectively. Micrographs of the coating cross-sections indicated that coating porosity (as-polished, not shown) did not increase significantly after heat treatment at 350-400 °C, Overall, the mechanical and microstructural characterization demonstrated that coatings heat treated for 1 h at 350-400 °C displayed acceptable strength and ductility.

Quantitative adhesion tests were conducted via ASTM E8 at different annealing conditions to validate the ASTM C633 testing. There was no generally difference among failure mechanism among the different coatings as a result of the annealing, as they failed within the coatings, and not at the interface (Figure 7); the coupons shown therein had an average adhesive strength of 67±5 MPa.

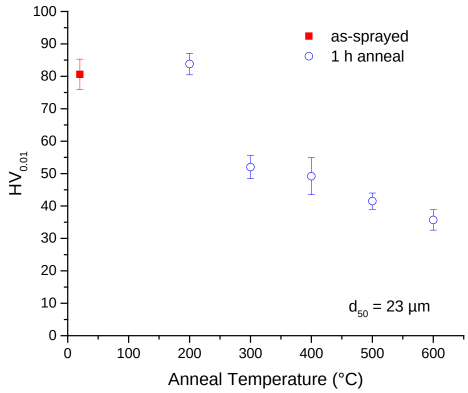

Figure 5: Coating hardness as a function of annealing temperature

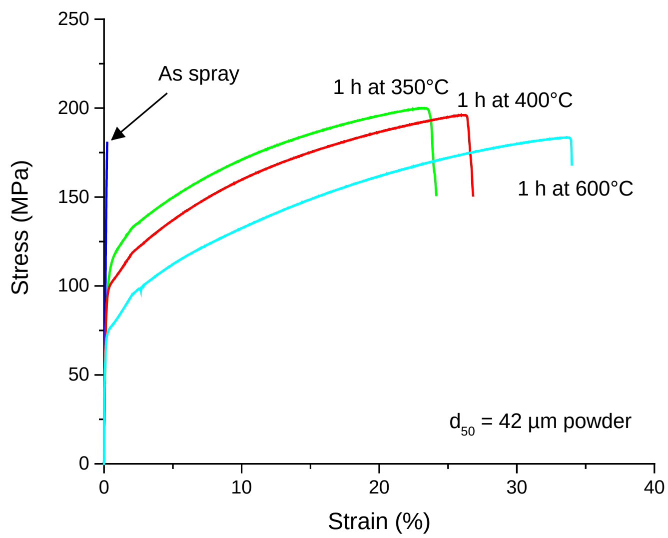

Figure 6: Coatings Stress Strain curves for different annealing temperature

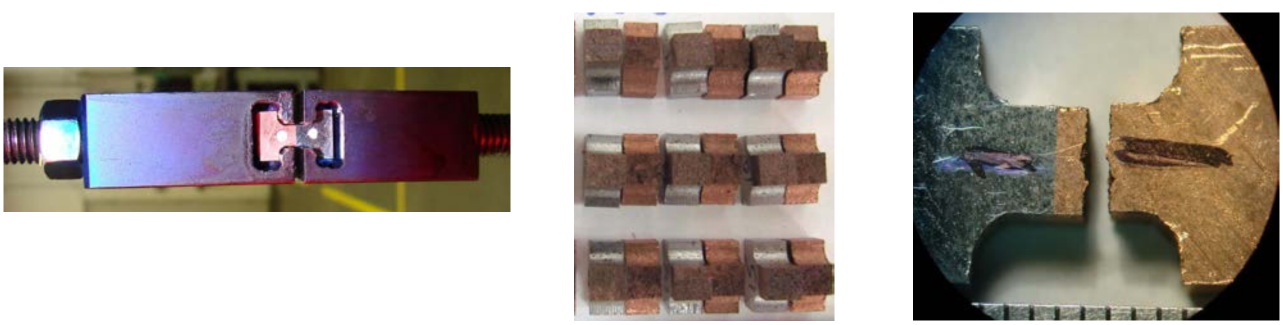

Figure 7: Adhesion testing conducted via modified ASTM E8 on coupons annealed to 350°C: (a)Coupon in Holder, (b) End-on view showing multiple fractures in coatings, and (c) side-on view showing fracture in coating.

Following this optimisation process, the reference cold-spray coating system was defined with the following parameters:

- 10-70 µm spherical low oxygen copper powder;
- 25.4 mm min. thick A516 grade 70 steel, grit blasted with 24 grit to remove millscale;
- 100 µm bond coat, applied with He-spray at 5 MPa and 800 °C,
- 3 mm top coat, applied with N_2-spray at 5 MPa and 800 °C, and
- Post-deposition heat treatment at 350°C for 1 hour.

As noted above, larger plates were produced (A516 grade 70, 150 mm x 150 mm x 38 mm plates fixed into a rotating 560 mm Ø sample holder seen in Fig 4 (b) for conditions validation and external performance testing, such as corrosion behaviour. Representative plates are shown in Figure 8.

(a) (b) (c)

Figure 8: A516 plate (a) as-sprayed plate side (b) as-sprayed coated surface (c) coating after machining

4. Coating Validation and Scale-Up

The cold spray process was validated many times on larger coupons representative of UFC materials and shapes. The effect of a curved substrate surface on the coating properties was investigated through the spraying of the reference coating on a A106 schedule C steel pipe segment (508 mm x 406 mm x 38 mm) fixed on a turntable, Figure 9. Metallographic observations of the coating confirm a fully dense microstructure similar to the planar samples previously produced.

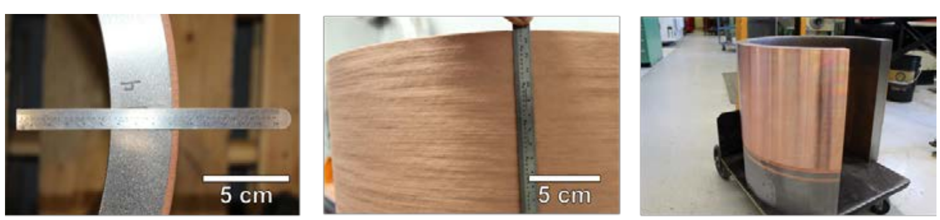

(a) (b) (c)

Figure 9: Coated pipe segment (a) pipe cross-section (b) as-sprayed surface and (c) coating after machining (a whole section was cut for analysis)

The coating process was then adjusted for further scale-up and changes in part geometries. Substrate handling and preparation steps were adapted (lift system, portable grit blast) and the powder feedrate was increased to improve productivity. He gas consumption was reduced by the use of a smaller diameter nozzle optimized for He-spray. The initial reduction in coating adhesion (to around 30 MPa) observed after this modification was attributed to a lower substrate temperature caused by less gas flow through the smaller diameter nozzle as well as an increased deposition rate of coating per pass. As such, an additional step of substrate preheating was added to the process and the rotation speed of the samples was adjusted to recover coating adhesion. Two hemispherical heads were produced. Adjustment of robot pattern and coating steps ensured complete coverage of the hemispherical head surfaces. One hemispherical head was cut to validate coating uniformity (Figure 10) while the other head was CNC machined for demonstration purpose.

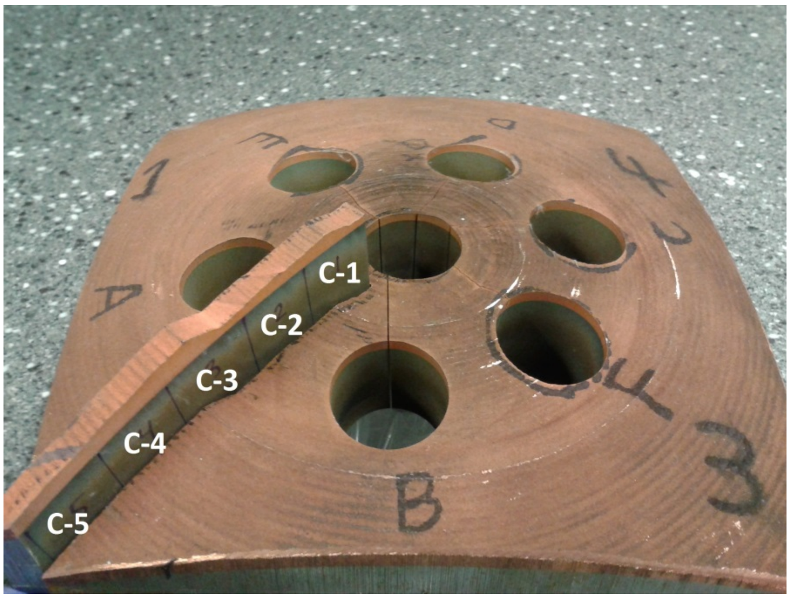

Figure 10: Section of the hemispherical head, illustrating the location of the samples extracted for characterisation

5. Process Demonstration

Process capability was demonstrated through pre-prototyping activities. A subsized container (Figure 11) was first produced, principally to develop the process transition from the cylindrical section to the hemispherical cap.

A full sized lower assembly (full part length of 2270 mm) was subsequently coated. The setup for coating the subsized assembly and full sized lower assembly, shown in Figure 12, employed a horizontal frame with motorized rollers to rotate the assemblies.

Subsized and full sized assemblies presented large surfaces to coat, requiring spraying over multiple work days. Restarting procedures were developed to account for surface preparation and blending/joining of the coatings deposited on previous sections. The spray pattern was modified to produce a taper at the edge of the each day's section in order to ensure smooth transition between sections. The overlapping copper region was grit blasted at the same time as the new section to cover prior to spraying. Post deposition microstructural observations of development coupons did not show any coating variation in the transition regions. Figure 12 shows the coating of the full sized lower assembly and the container after machining.

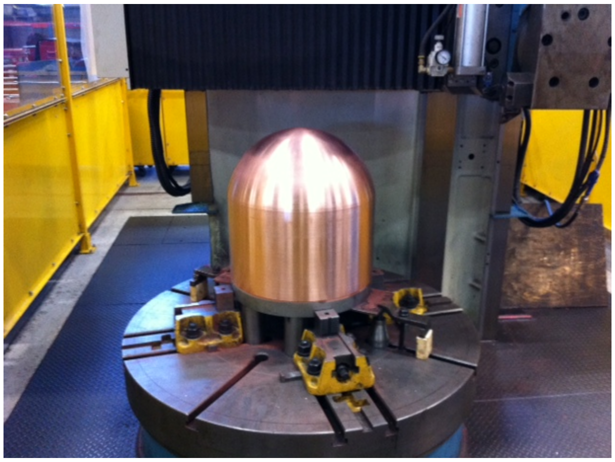

Figure 11: Coated and machined subsized container representing a full diameter lower section of the canister (i.e., full size hemispherical head and weld transition) with a truncated cylindrical body (560 mm Ø × 620 mm part length)

(a) (b) (c)

Figure 12: Full sized lower assembly (a) after coating of two sections, (b) after coating of entire lower assembly, and (c) after machining of lower assembly.

The feasibility of producing a fully coated container was finally validated by the spraying of the closure weld area (Figure 13). The coated full sized lower assembly was laser welded to a coated hemispherical head. The full container was rotated and coating added on the closure zone using the reference parameters. A final machining provided an even surface along the cylindrical part of the container. It must be noted that further development is underway for closure zone spraying at lower rotating speed, in order to minimise impacts and stresses on used fuel bundles that would eventually be placed inside the closed container.

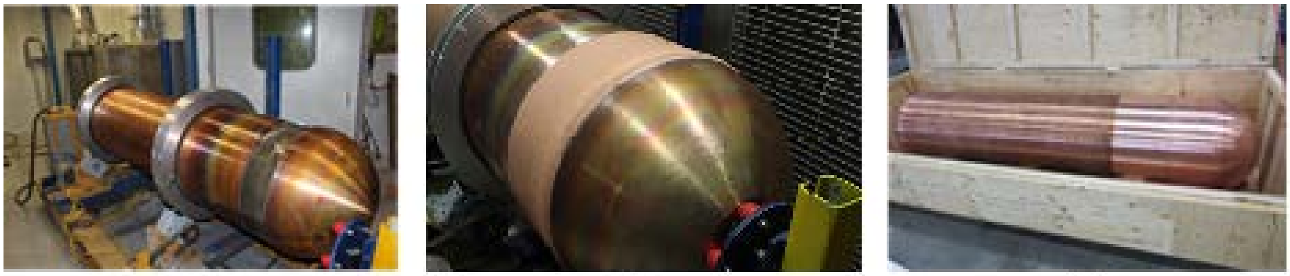

(a) (b) (c)

Figure 13: Full sized leading assembly: (a) installed with collars on roller frame prior to coating of the closure weld after its welding and machining, (b) after coating of the closure weld (c) after coating and machining of the closure weld.

6. Conclusions and Future Work

The successful application of the cold spray coating technology to full scale geometric representative UFC (carbon steel cylinder/hemispherical heads and weld closure zones) was demonstrated through activities involving (i) coating initial development, (iii) coating validation, and (iii) scale-up and pre-prototyping activities. Coating initial development included powder selection and cold spray/annealing parameters optimization for the establishment of reference process conditions. Coating quality and properties were then validated on UFC representative materials and shapes. Process scale-up necessitated process parameter adjustment as well as spray set-up and pattern development. Different prototyping activities ended up by the production of a fully coated full-sized container, the manufacturing steps being determined as (i) coating spraying and machining of an hemispherical head and lower assembly, (ii) joining of the two container sections through laser welding, (iii) coating spraying of the weld closure zone and (iv) final machining. Further development of the cold spray process for the coating of the weld closure zone within a clear operating window is currently underway.

7. References

[1] E. Irissou et al, “Review on Cold Spray Process and Technology: Part 1 – Intellectual Property”, Journal of Thermal Spray Technology, Vol. 17, Iss. 4, 2008, pp.495-511.

[2] Schmidt, T., Assadi, H., Gartner, F., Richter, H., Stoltenhoff, T., Kreye, H., and Klassen, T. (2009). From particle acceleration to impact and bonding in cold spraying. J. Therm. Spray Technol., 18 5-6, 794-808

[3] M. Grujicic et al, “Analysis of the impact velocity of powder particles in the cold-gas dynamic-spray process”, Materials Science and engineering A, Vol. 368, Iss. 1-2, 2004, pp.222-230.

[4] H. Assadi et al, “Bonding mechanism in cold gas spraying”, Acta Materialia, Vol.51, Iss.15, 2003, pp.4379-4394.